Targeted gene deletion in *Candida parapsilosis* demonstrates the role of secreted lipase in virulence

Attila Gácser,[1] David Trofa,[1] Wilhelm Schäfer,[2] and Joshua D. Nosanchuk[1,3]

[1]Department of Medicine, Division of Infectious Diseases, Albert Einstein College of Medicine, Yeshiva University, New York, New York, USA.
[2]Department of Molecular Phytopathology and Genetics, Biocenter Klein Flottbek, University of Hamburg, Hamburg, Germany.
[3]Department of Microbiology and Immunology, Albert Einstein College of Medicine, Yeshiva University, New York, New York, USA.

Candida parapsilosis **is a major cause of human disease, yet little is known about the pathogen's virulence. We have developed an efficient gene deletion system for *C. parapsilosis* based on the repeated use of the dominant nourseothricin resistance marker (*caSAT1*) and its subsequent deletion by FLP-mediated, site-specific recombination. Using this technique, we deleted the lipase locus in the *C. parapsilosis* genome consisting of adjacent genes *CpLIP1* and *CpLIP2*. Additionally we reconstructed the *CpLIP2* gene, which restored lipase activity. Lipolytic activity was absent in the null mutants, whereas the WT, heterozygous, and reconstructed mutants showed similar lipase production. Biofilm formation was inhibited with lipase-negative mutants and their growth was significantly reduced in lipid-rich media. The knockout mutants were more efficiently ingested and killed by J774.16 and RAW 264.7 macrophage-like cells. Additionally, the lipase-negative mutants were significantly less virulent in infection models that involve inoculation of reconstituted human oral epithelium or murine intraperitoneal challenge. These studies represent what we believe to be the first targeted disruption of a gene in *C. parapsilosis* and show that *C. parapsilosis*–secreted lipase is involved in disease pathogenesis. This efficient system for targeted gene deletion holds great promise for rapidly enhancing our knowledge of the biology and virulence of this increasingly common invasive fungal pathogen.**

Introduction

Candida parapsilosis is currently the second most common cause of invasive candidiasis worldwide (1–5). The fungus is particularly associated with disease in premature infants and immunocompromised adults and is a major cause of nosocomial infection in intensive care units (6, 7). Despite increasing clinical importance, little is known about the genetic basis of fungal virulence traits that enable *C. parapsilosis* to cause disease. Hence virulence factors of *C. parapsilosis* need to be identified in order to develop more effective therapy against this pathogen.

Secretion of hydrolytic enzymes such as secreted aspartic proteinases and lipases (8) have been associated with *Candida albicans* virulence (8–12). Putative roles of microbial extracellular lipases include the digestion of lipids for nutrient acquisition, adhesion to host cells and tissues, synergistic interactions with other enzymes, unspecific hydrolysis, initiation of inflammatory processes by affecting immune cells, and self defense by lysing the competing microflora (11). Two lipase genes, *CpLIP1* and *CpLIP2*, have been identified in *C. parapsilosis*. However, when *CpLIP1* and *CpLIP2* were expressed in *Saccharomyces cerevisiae* (13) and *Pichia pastoris* (14), only *CpLIP2* coded for an active protein. *CpLIP2* is homologous to 11 lipases produced by *C. albicans* (42%–61% sequence identity), and the alignments suggest that this enzyme belongs to what we believe to be a new family of fungal lipases (9, 13).

We have previously shown that lipase inhibitors significantly reduce tissue damage during infection of reconstituted human tissues (15). These findings support our hypothesis that *C. parapsilosis CpLIP2* is involved in pathogenesis. The aim of this study was to develop a transformation system for *C. parapsilosis* based upon the FLP-mediated *caSAT1* resistance marker recycling (16) and conferring resistance to nourseothricin (Nou). We constructed *CpLIP1-CpLIP2* knockout (KO) mutants and reconstituted strains to further explore the role of lipase in *C. parapsilosis* pathogenesis.

Results

Disruption of the lipase locus in C. parapsilosis by SAT1 flipper to generate lipase-negative mutants. Since the lipase genes *CpLIP1* and *CpLIP2* are adjacent, we designed a gene-disruption construct to target the whole lipase locus in the *C. parapsilosis* genome to generate a lipase-negative strain. The strategy for gene disruption using the *SAT1* flipper is outlined in Figure 1A. The *SAT1* flipper cassette contains the *caSAT1*, the *C. albicans*–adapted Nou resistance marker, and the site-specific recombinase gene (*caFLP*) under the control of a maltose inducible maltose promoter (*MAL2*). The cassette is flanked by FRT sequences to provide the minimal FLP recombination target sites. The *C. parapsilosis* clinical isolate GA1 was transformed by electroporation with a linear DNA fragment, in which 2,701 bp were replaced by the insertion of the *SAT1* cassette. The cells treated with electric pulse were incubated at 30°C in yeast extract/peptone/dextrose (YPD) liquid medium containing 1 M sorbitol without shaking prior to plating on Nou agar. After 2 days of incubation, Nou-resistant (Nou^R) colonies were present on the selection plate (Figure 1C) and could be picked and used to prepare cultures for DNA isolation. The Nou^R mutants were examined by Southern blot hybridization in order to demonstrate homologous integration. Figure 1B shows the Southern blot

Nonstandard abbreviations used: HE, heterozygous; Nou, nourseothricin; Nou^R, Nou-resistant; Nou^S, Nou-sensitive; RE, reconstituted; YNB, yeast nitrogen base (medium); YPD, yeast extract/peptone/dextrose (medium).

Conflict of interest: The authors have declared that no conflict of interest exists.

Citation for this article: *J. Clin. Invest.* **117**:3049–3058 (2007). doi:10.1172/JCI32294.

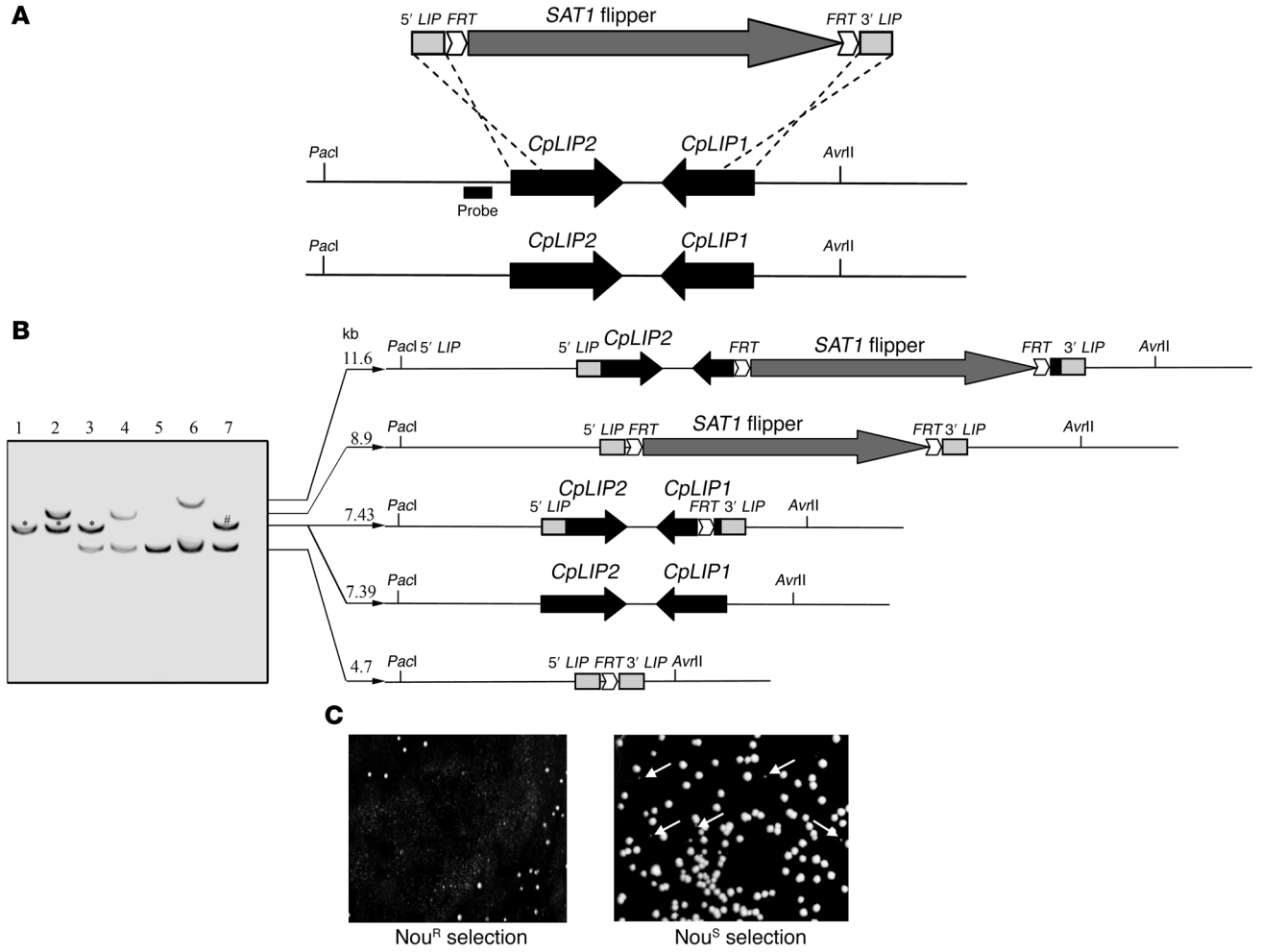

Figure 1
Gene deletion in *C. parapsilosis*. (**A**) Design of gene targeting for the *C. parapsilosis* lipase locus showing the *SAT1* flipper cassette with the homologous *C. parapsilosis* lipase fragments 5′ *LIP* and 3′ *LIP* as well as the FLP recombination target sequences (*FRT*). The probe used to verify correct integration and deletion of the SAT1 flipper by Southern blot hybridization is represented by a black bar. (**B**) Southern blot hybridization analysis of genomic DNA (*Pac*I, *Avr*II, double digested) isolated from the WT GA1 (lane 1), the heterozygous mutant *CpLIP1-2*/Δ*cplip1-2:SAT1-FLIP* (HebFLP) before FLP activation (lane 2), the heterozygous mutant *CpLIP1-2*/Δ*cplip1-2:FRT* (HE) after excision of *SAT1* flipper cassette (lane 3), the homozygous mutant Δ*cplip1-2*/Δ*cplip1-2:SAT1-FLIP* (KobFLP) before FLP activation (lane 4), the homozygous mutant Δ*cplip1-2*/Δ*cplip1-2:FRT* (KO) after excision of *SAT1* flipper cassette (lane 5), the reintegration mutant Δ*cplip1-2*/Δ*cplip1-2*/*CpLIP2:SAT1-FLIP* (RebFLP) before FLP activation (lane 6), and the reconstituted mutant Δ*cplip1-2*/Δ*cplip1-2*/*CpLIP2:FRT* (RE) after FLP activation (lane 7). Diagrams of the structures and size of the hybridization fragments are shown at right. (**C**) Nou selection of *caSAT1*-containing (Nou^R) transformants (left) and screening for Nou^S colonies after FLP activation (right). Arrows indicate small Nou^S colonies.

hybridization with a probe that localized outside of the homologous regions (Figure 1A). Of the 24 transformants analyzed, 3 showed correct integration of the cassette into the lipase locus. The Southern blot results showed that the *C. parapsilosis* genome contained 2 copies from this particular locus (Figure 1B, lane 2). The homologous integrated heterozygous mutants (HebFLP) were inoculated into yeast nitrogen base (YNB) medium containing maltose in order to induce FLP-mediated excision of the *caSAT1* resistance gene. In contrast to *C. albicans* (16), *C. parapsilosis MAL2* promoter induction was found only in YNB-maltose medium and not in YPD, suggesting that the *MAL2* promoter derived from *C. albicans* is more substrate specific in this heterologous system. After 24 hours of induction, approximately 200 cells were plated on the YPD plate containing 20 μg/ml Nou. The Nou-sensitive (Nou^S) cells grew more slowly and formed smaller colonies in comparison with Nou^R colonies (Figure 1C). Southern blot analysis showed that all of the Nou^S clones lacked the resistance marker (Figure 1B, lane 3). Three independent heterozygous FLP-activated clones were used in the second round of transformation in order to inactivate the remaining WT locus. We analyzed 24 mutants from each transformation and found 2 independent homozygous mutants that showed correct integration (Figure 1B, lane 5). The *MAL2* activation and the excision of the resistance marker was done as described in the first transformation.

Construction of C. parapsilosis CpLIP2-reconstituted strain. To show that the mutant phenotype was caused by the lipase locus deletion, we reintroduced the *CpLIP2* gene into its original genomic locus. The pCPLRE vector was designed to recover WT lipolytic activity in the lipase-negative mutants. The homozygous mutants were elec-

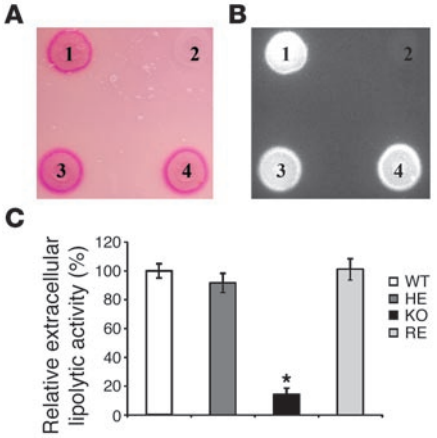

Figure 2
Lipase activity of *C. parapsilosis* WT and lipase mutants. (**A**) Effect of *C. parapsilosis* WT and lipase mutants on rhodamine B–FCS agar plate. Lipolytic activities are demonstrated by the red-stained regions around the colonies. 1, WT strain; 2, homozygous mutant; 3, heterozygous mutant; and 4, reconstituted mutant. (**B**) Rhodamine B–FCS agar plate irradiated with UV light. Fluorescent halos indicate lipolytic activity. The experiment was performed 3 times with similar results. (**C**) Relative extracellular lipolytic activity of *C. parapsilosis* WT, heterozygous *CpLIP1-2*/Δ*cplip1-2* (HE), homozygous Δ*cplip1-2*/Δ*cplip1-2* (KO), and reconstituted Δ*cplip1-2*/*CpLIP2* (RE) mutants. Lipolytic activities of supernatants of overnight cultures in YNB–olive oil medium were measured using paranitrophenyl palmitate. Error bars indicate SD. **P* < 0.0001 (ANOVA).

troporated with the linear DNA fragment that contained the complete *CpLIP2* gene, including upstream and downstream regions with the *CpLIP1* gene, amplified from the WT strain. It was previously shown that *CpLIP2* encodes functional lipase protein, while *CpLIP1* does not appear to be active (13). After transformation, we picked 48 colonies to analyze via Southern blot analysis and found 16 colonies with the correct integration. The *SAT1* flipper was then activated and the resistance marker was excised, resulting in the reconstituted strain (RE; Δ*cplip1-2/CpLIP2*), a derivate of strain KO (Δ*cplip1-2*/Δ*cplip1-2*), in which the WT lipase locus was reintroduced into the deleted locus (Figure 1B, lanes 6 and 7).

Lipolytic activity of the C. parapsilosis WT, lipase minus, and RE strains. The WT strain, the heterozygous mutant (HE; *CpLIP1-2*/Δ*cplip1-2*), and the RE mutant exhibited similar lipolytic activities as demonstrated by the red-stained regions around the colonies grown on YNB–FCS–rhodamine B plates (Figure 2A) and the intense fluorescence under UV light (Figure 2B). The homozygous lipase-negative mutants had no detectable activity in the plate assay (Figure 2, A and B).

Secreted lipolytic activities were also tested in supernatants from cells incubated for 24 hours at 37°C in YNB liquid media using olive oil as a carbon source and in lipid-rich media containing 5% intralipid solution. The supernatants obtained from the examined homozygous KO mutant exhibited almost no residual activity ($P = 0.0001$) (Figure 2C). Although the HE mutant produced a lipolytic activity slightly lower than that of the WT strain, the difference was not statistically significant ($P = 0.08$). The activity levels of RE strains were equivalent to WT.

Growth of the C. parapsilosis lipase-negative and RE strains in different liquid media. Growth rates in liquid YPD and YNB media and 2 different lipid media (YNB–olive oil and intralipid) were examined. There were no significant differences in growth in the strains in YPD or YNB (Figure 3, A and B). However, there was an 80% reduction in growth in the lipase-negative strain in YNB–olive oil medium compared with WT (7.3×10^7 and 2×10^7 cells/ml, respectively; $P < 0.05$) (Figure 3C). The lipase-negative mutant cell density plateaued by 96 hours and never reached more than 30% that of the WT strain (data not shown). Similarly, the KO strain stagnated

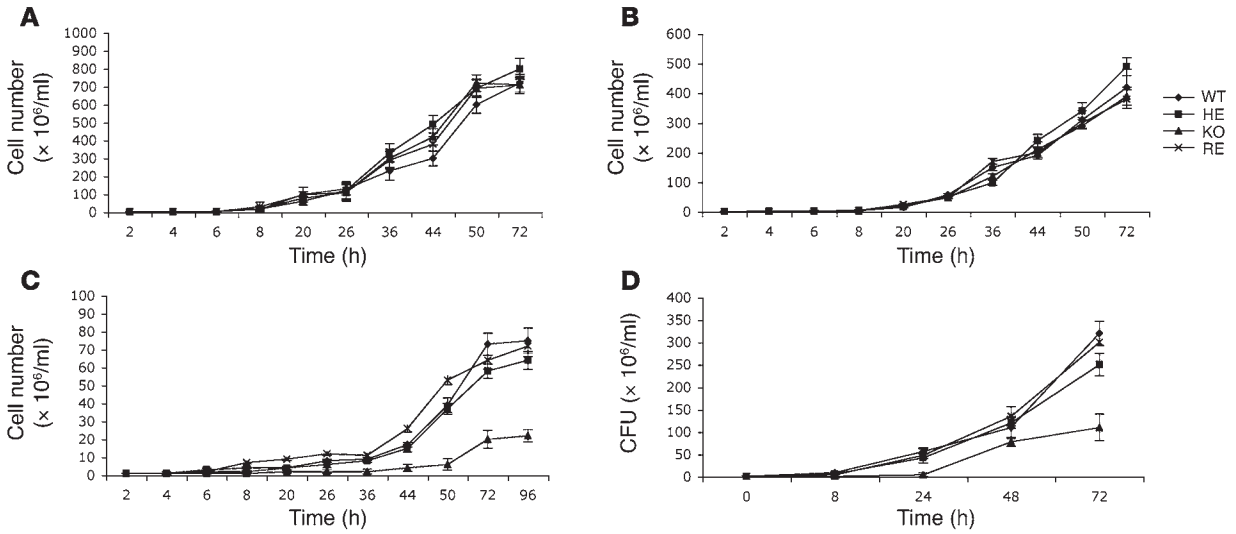

Figure 3
Growth curves of *C. parapsilosis* WT and lipase mutants in YPD, YNB, YNB–olive oil, and in YNB-intralipid media. Growth curves of the WT strain and heterozygous *CpLIP1-2*/Δ*cplip1-2*, homozygous Δ*cplip1-2*/Δ*cplip1-2*, and reconstituted Δ*cplip1-2*/*CpLIP2* mutants in YPD (**A**), YNB (**B**), and YNB–olive oil (**C**) media. (**D**) CFU in YNB-intralipid solution. Error bars indicate SD. The experiment was repeated, and similar results were found.

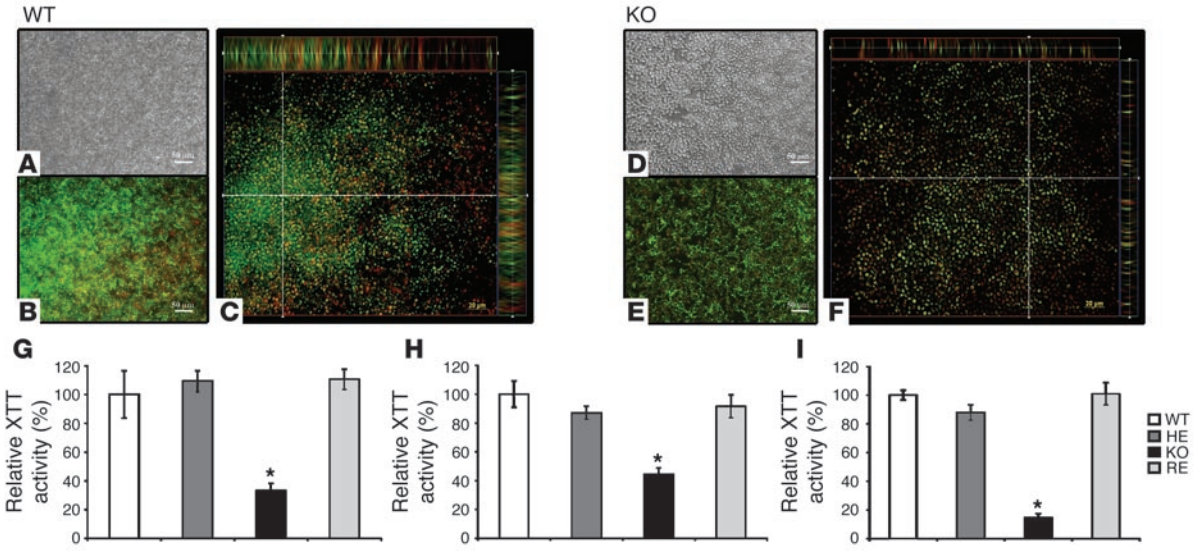

Figure 4
Comparison of biofilm formed by *C. parapsilosis* WT and homozygous Δ*cplip1-2*/Δ*cplip1-2*, heterozygous *CpLIP1-2*/Δ*cplip1-2*, and reconstituted Δ*cplip1-2*/*CpLIP2* mutants. (**A**) Light microscopy, (**B**) fluorescent microscopy, and (**C**) confocal microscopy images of WT biofilm on polyethylene surface after incubation for 48 hours at 37°C in YNB medium. The biofilm formed by the homozygous Δ*cplip1-2*/Δ*cplip1-2* mutant is shown by (**D**) light microscopy, (**E**) fluorescent microscopy, and (**F**) confocal microscopy. (**G**–**I**) Comparison of biofilm formed by *C. parapsilosis* WT and lipase mutants on different surfaces. Relative XTT activity of biofilm formed on (**G**) polyethylene, (**H**) silicone, and (**I**) polystyrene surfaces. XTT activity was measured at 492 nm. **P* < 0.02 (ANOVA). Error bars indicate SD. The experiment was repeated 3 times, and equivalent results were obtained. Scale bars: 50 μm (**A**, **B**, **D**, and **E**); 20 μm (**C** and **F**).

after 48 hours in YNB–intralipid medium (pH 5–6) (Figure 3D) and was only 34% that of WT after 72 hours (1.1×10^8 and 3.2×10^8 cells/ml, respectively; $P < 0.002$) (Figure 3D).

Comparison of biofilms formed by C. parapsilosis WT and lipase mutants on polystyrene surface. We measured *C. parapsilosis* biofilm growth on various surfaces. Preincubation of surfaces such as polystyrene, polyethylene, and silicone with FBS consistently produces more biofilm than incubation with PBS (17). We measured biofilm growth on FBS-treated surfaces using both an XTT assay and microscopy. *C. parapsilosis* WT was able to form biofilm on all 3 surfaces, but the metabolitic activity of the resultant biofilms was higher on polyethylene and on silicon surfaces in comparison with polystyrene (data not shown). Figure 4, A–F, illustrates microscopic analysis of biofilms obtained from *C. parapsilosis* WT and KO strains incubated on polyethylene surfaces in minimal YNB medium. Light microscopic analysis showed significant differences between biofilms formed by WT and lipase-negative strains. Individual fungal cells could be distinguished in the case of lipase mutants (Figure 4D), while WT fungal cells were undistinguishable due to aggregation (Figure 4A). Fluorescent micrographs showed intense green fluorescence resulting from concanavalin A (ConA) binding to polysaccharides coating the cell walls of the yeast, while the red color resulted from FUN-1 staining localized in dense aggregates in the cytoplasm of metabolically active cells. WT biofilm showed more intense overall fluorescent staining (Figure 4B) than the biofilm formed by lipase-negative cells (Figure 4E). Vertical (*x*-*z* axes) sectioning of 3-dimensional reconstructed images (Figure 4, C and F) showed that *C. parapsilosis* WT biofilm consisted of multiple layers of metabolically active cells represented by yellow dual staining (Figure 4C). In contrast, KO mutant biofilm had significantly less thickness and complexity. Using the XTT assay, we found that the homozygous KO mutants had significantly ($P < 0.002$) lower metabolic activity than WT cells on polyethylene (Figure 4G), silicone (Figure 4H), and polystyrene (Figure 4I) surfaces. The biofilm formed by the HE strain had slightly reduced metabolic activity, but it was not significantly different from WT.

Histopathological analysis of RE human oral epithelium infected with C. parapsilosis lipase-negative mutants and WT. The RE oral epithelial tissues were fixed, sectioned, and stained 48 hours after infection. Dramatic histopathological alterations occurred after challenge with *C. parapsilosis* WT, HE, and RE strains due to the invasion of numerous yeast cells into tissue (Figure 5, C–F, I, and J). With lipase-producing *C. parapsilosis*, there was marked attenuation of the epithelium (atrophy), loss of epithelial whorls, inter- and intracellular edema (Figure 5C, middle inset, and Figure 5E, middle and lower insets), and increased apoptotic cells (Figure 5C, top inset, and Figure 5E, top inset). In addition, basal cells were low cuboidal and clefting (Figure 5C, lower inset). Irregular cleft formation was also apparent between cells in the upper layers, and the epithelial surface was moderately disrupted. In contrast, few lipase-negative yeast were found attached to the tissue, and the epithelium appeared similar to control tissue, except that the superficial cells were slightly flattened and the tissue surface was irregular (Figure 5, G and H). To quantify cell injury, we compared the levels of lactate dehydrogenase (LDH) released into culture supernatant after *C. parapsilosis* WT, HE, KO, and RE strains were exposed to RE oral epithelium for 48 hours (Figure 5K). The LDH results correlated with the tissue damage seen by light microscopy. WT, HE, and RE strains had the highest level of LDH and tissue damage, whereas the homozygous lipase-negative strain had significantly lower levels of LDH and less damage.

Phagocytosis of C. parapsilosis by macrophages. We compared the phagocytosis of WT and lipase mutants by macrophage-like J774.16 and RAW 264.7 cells using an acridine orange staining assay (Figure 6, A and B). In each condition, homozygous KO mutant cells were ingested more efficiently (Figure 6, C and D). The phagocytic indices

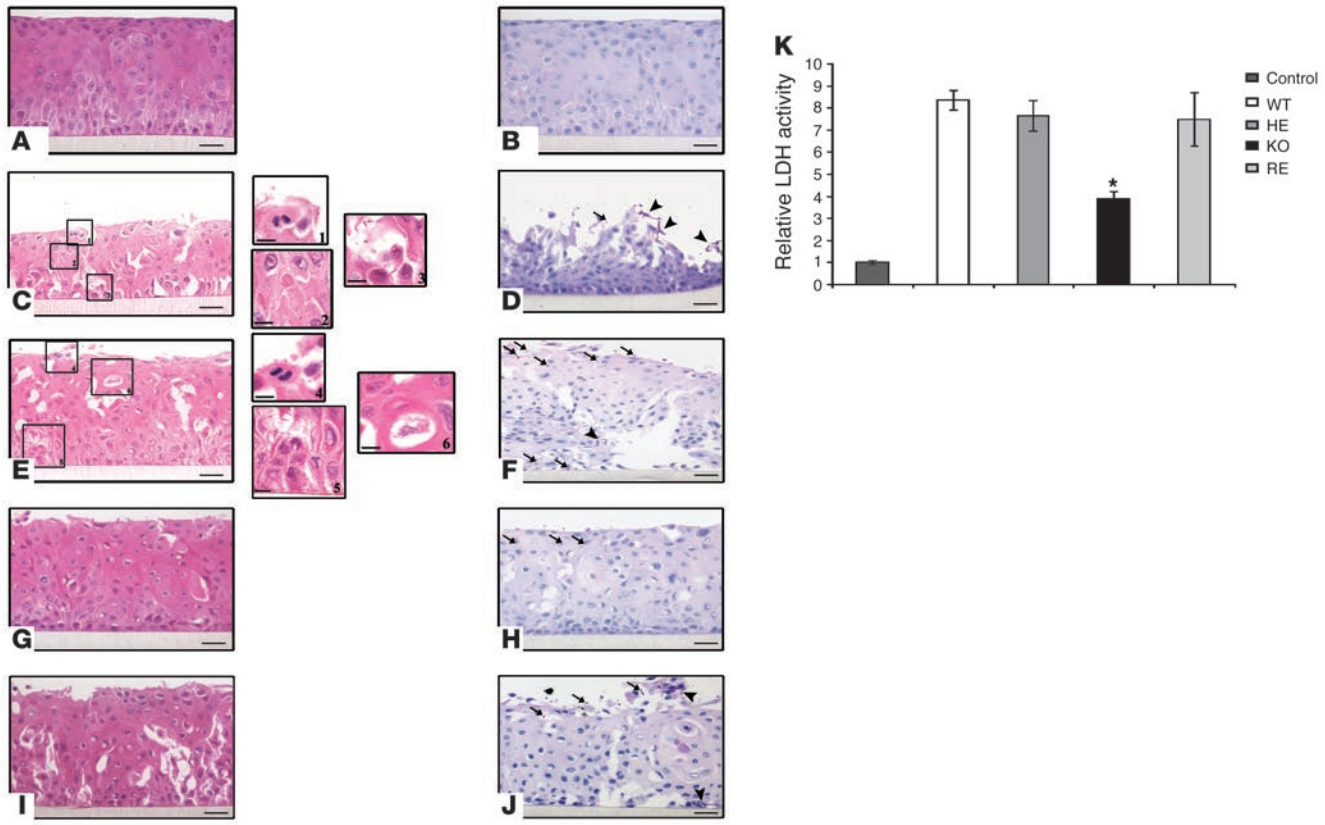

Figure 5
Reconstituted human oral epithelium at 48 hours infected with *C. parapsilosis* WT. (**A** and **B**) Uninfected control tissues, (**C** and **D**) WT, (**E** and **F**) heterozygous mutant *CpLIP1-2*/Δ*cplip1-2*, (**G** and **H**) homozygous mutant Δ*cplip1-2*/ Δ*cplip1-2*, and (**I** and **J**) reconstituted Δ*cplip1-2*/*CpLIP2*. Insets show histopathological alterations. Top insets in **C** and **E** show apoptotic cells; middle insets in **C** and **E** show intercellular edema; bottom inset in **C** shows cleft formation and tissue separation; and bottom inset in **E** shows vacuolization. Left panels demonstrate hematoxylin and eosin staining, and right panels periodic acid Schiff staining. Arrows indicate yeast cells, and arrowheads indicate pseudohyphae. Scale bars: 10 μm (**A**–**J**); 5 μm (all insets). (**K**) Relative LDH measured in the tissue culture supernatant by reconstituted human oral epithelium after 48 hours of coculture with WT, heterozygous mutant *CpLIP1-2*/Δ*cplip1-2,* homozygous mutant Δ*cplip1-2*/ Δ*cplip1-2*, and reconstituted mutant Δ*cplip1-2*/*CpLIP2*. Error bars indicate SD. The assay was repeated 3 times. *$P < 0.02$ (ANOVA).

increased from 5.8 to 7.1 (21.3% increase) and from 3.9 to 5.2 (33% increase) comparing WT and homozygous KO cells, respectively. Phagocytosis of HE and RE strains was similar to that of WT.

Phagocytic killing activity. Killing of intracellular *C. parapsilosis* cells was measured by CFU determination after coculture with macrophage. Both macrophage-like cell lines were able to kill *C. parapsilosis* cells efficiently. However, significantly more lipase-negative cells were killed compared with WT, with 72% versus 40% killing in J774.16 and 74% versus 46% in RAW 264.7, respectively (Figure 6, E and F). The killing of HE strains was similar to that of WT strains. The results suggest that the secreted lipases can play an important role in the intracellular survival within macrophages.

Endothelial cell damage assay. During the process of hematogenous dissemination, *Candida* cells must first cross the endothelial cell lining of the vasculature to invade tissue parenchyma. One mechanism by which the organism may escape from the vascular compartment is by causing endothelial cell injury (18). We tested the ability of lipase mutants to damage monolayers of HUVECs using a LDH release assay. We used *C. albicans* SC5314 strain as a positive control, since it is known that *C. albicans* causes endothelial cell injury in vitro and in vivo. No significant differences were seen between HUVEC death caused by *C. parapsilosis* WT and by lipase mutants (Figure 7). However, the level of HUVEC lysis caused by *C. parapsilosis* was 3 times less than that caused by *C. albicans*.

Analysis of the lipase-negative mutants in mouse infection models. To simulate peritonitis, Balb/c mice were inoculated intraperitoneally with either WT or lipase mutants, and fungal burdens were studied. The homozygous lipase-negative mutants were significantly less virulent, as demonstrated by the reductions in liver, kidney, and spleen CFUs compared with WT 2 days after infection ($P \leq 0.0049$; Figure 8A). On day 4 following infection, yeast cells were detectable from organs of mice infected with WT, HE, and RE strains, but no detectable yeast cells were found in mice inoculated with the homozygous lipase-mutant strain (Figure 8B). However, *C. parapsilosis* yeast could not be recovered on day 7 from any of the organs of mice inoculated with WT, HE, or RE strains. There were no differences in CFU counts or survival in the intravenous infection model (Figure 8C).

Discussion

In recent years, *C. parapsilosis* has risen to be the second most commonly isolated fungal organism in blood cultures (2, 3, 19, 20). *C. parapsilosis* is of special concern in critically ill neonates, causing

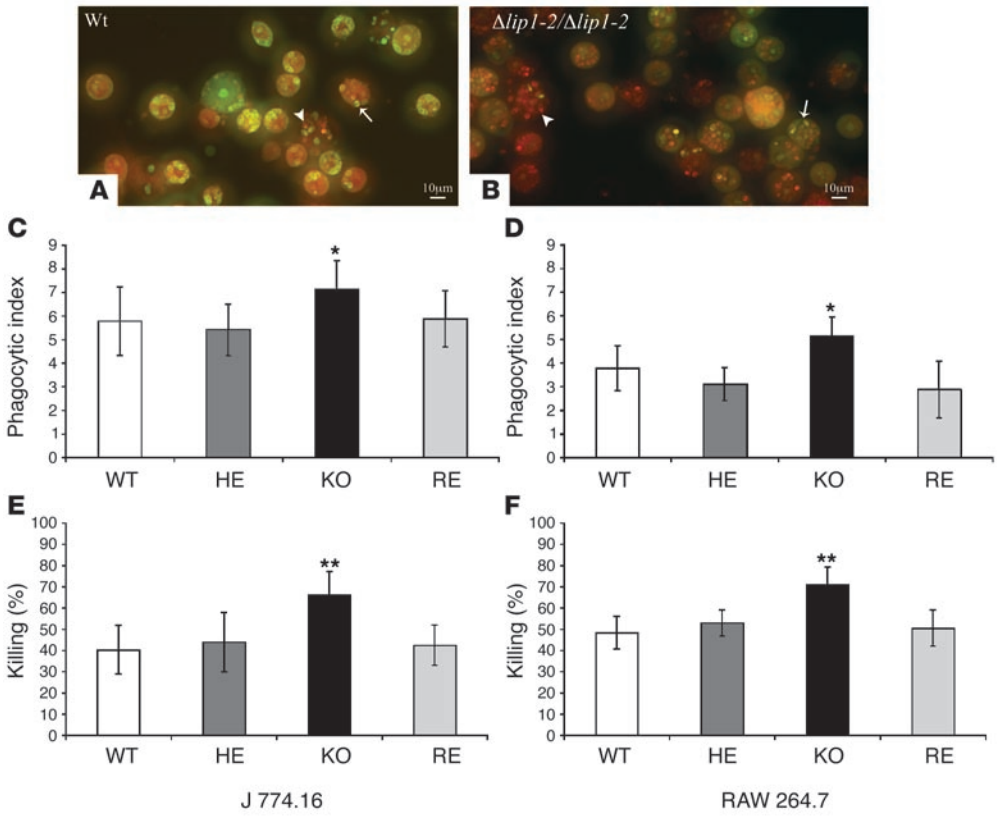

Figure 6
Phagocytosis and killing of *C. parapsilosis* cells by macrophage-like cell lines J774.16 and RAW 264.7. Fluorescent microscopic image of phagocytosis of *C. parapsilosis* (**A**) WT cells and (**B**) Δ*cplip1-2*/ Δ*cplip1-2* lipase-negative cells by J774.16 macrophages. Dead *C. parapsilosis* (arrowheads) show bright red and yellow fluorescence. Living cells show green fluorescence (arrows). Scale bars: 10 μm. (**C** and **D**) Phagocytosis by (**C**) J774.16 and (**D**) RAW 264.7 macrophage-like cells. Bars represent the mean measurements from 3 wells (at least 5 fields each). $^{*}P < 0.02$. (**E** and **F**) Intracellular killing of *C. parapsilosis* WT and mutants by macrophage-like cells. Killing by (**E**) J774.16 and (**F**) RAW 264.7 macrophage-like cells. Bars represent mean percentage of killing determined by CFU counts. Error bars indicate SD. $^{**}P < 0.01$ (ANOVA).

more than a quarter of all invasive fungal infections in low-birth-weight infants in the United Kingdom (7) and North America (6) and is a leading cause of neonatal mortality. In vitro *C. parapsilosis* proliferates in high concentrations of glucose and lipids and has a propensity to form biofilms on synthetic materials (21). Molecular genetic studies of *C. parapsilosis* have been hindered by the aneuploidy of the organism (22) and the lack of a characterized sexual cycle. A transformation system based on the complementation of a galactokinase-deficient mutant of *C. parapsilosis* by the homologous gene (*GAL1*) has been described, but it lacks efficiency and cannot be used to inactivate target genes in prototrophic WT strains (23). Our studies demonstrate that the *SAT1* flipper cassette is an efficient tool to generate homozygous KO mutants in *C. parapsilosis*. Although we previously showed that the dominant selection marker MPA^R is useful for *C. parapsilosis* transformation (24), the Nou selection has several advantages: transformants grow much more rapidly, the number of spontaneously resistant colonies is reduced, and the homologous recombination efficiency is much higher. In *C. albicans*, the *MAL2* promoter may lack specificity and only requires a 6-hour incubation in YPD medium to induce the FLP-mediated excision of the resistance marker (16). In our study, induction of the *MAL2* promoter to obtain Nou^S derivatives required a 24-hour incubation in YNB-maltose medium. This study and previous data (24) demonstrate that there are at least 2 independent dominant selection markers, MPA^R and *SAT1*, available for genetic manipulation in *C. parapsilosis*. Additionally, the fact that the KO cassette contains only heterogenous sequences derived from *C. albicans* and *Streptomyces noursei* reduces the possibility of recombinations into nontarget sequences. The marker recycling makes it possible to generate mutants that differ from the parental strain only by the absence of the target gene.

The pathogenesis of *Candida* infections is facilitated by a number of virulence factors. Examples include adherence to host cells and secretion of hydrolytic enzymes such as proteases, phospholipases, and lipases (12, 25). Although secreted lipolytic enzymes of pathogenic bacteria have been proposed as virulence factors (26), little is known about the involvement of lipases in fungal disease. As confirmed by subsequent Southern blotting analysis, we successfully disrupted the lipase locus containing the *CpLIP1* and the *CpLIP2* genes in the *C. parapsilosis* clinical isolate GA1. The reduced growth capability of the homozygous mutant in lipid-containing media (YNB–olive oil and YNB-intralipid) suggests that the presence of extracellular lipase activity is necessary for optimal growth in such media and that the product of the gene might play an important role in digesting lipids for nutrient acquisition. This is particularly important since lipid-rich total parenteral nutrition is commonly administered to low-birth-weight neonates. The use of central venous catheters to deliver parenteral nutrition solutions is a well established risk factor for invasive candida infections, although no significant difference in the frequency of central venous catheter use between infants infected with *C. parapsilosis* and those infected with *C. albicans* has been noted (6, 7, 27). Interestingly, medium-chain-length lipid emulsions can increase *C. albicans* growth rates (28), which can be linked to the production of lipases. In this study the growth of the homozygous lipase-negative strain was consistently retarded in both YNB–olive oil and YNB-intralipid media. Thus extracellular lipase proteins seem to be necessary for optimal proliferation of *C. parapsilosis* in lipid solutions, suggesting that lipases are colonization factors facilitating nutrient acquisition and growth in a lipid-rich environment. Hence the *CpLIP2* and the encoded enzyme are potential targets for the inhibition of *C. parapsilosis* proliferation, especially in lipid emulsions.

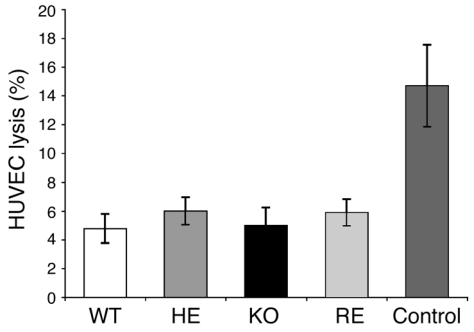

Figure 7
Endothelial damage assay of *C. parapsilosis* WT, heterozygous mutant *CpLIP1-2*/Δ*cplip1-2*, homozygous mutant Δ*cplip1-2*/Δ*cplip1-2*, and reconstituted Δ*cplip1-2*/*CpLIP2* mutant. *C. albicans* SC5314 cells were used as a positive control. HUVEC lysis was measured after 8 hours by LDH assay. Error bars indicate SD. The assay was repeated 3 times.

As only 2 lipase genes are known in *C. parapsilosis,* and only the *CpLIP2* produces functional enzyme, we examined the residual lipolytic activity from homozygous gene–deleted mutants. However, the recent genomic DNA sequencing project results suggest that 2 additional *LIP* genes may exist in *C. parapsilosis*. It is possible that expression of these genes under specific conditions may account for the late growth in olive oil medium or even in vivo. Nevertheless, supernatants of the lipase-negative mutants cultured in YNB–olive oil and YNB-intralipid solutions showed almost no lipase activity. Additionally, we were able to restore the WT phenotype after reinserting one copy of the *CpLIP2* gene. To verify the extracellular lipase assay results, the growth of WT and mutants were examined on plates containing rhodamine B and olive oil (29). The WT strain had a well defined red-colored area around the colonies with orange fluorescence under UV light indicative of lipolytic activity, while no such coloration occurred with the lipase-negative strains, suggesting the successful elimination of extracellular lipase activity.

Biofilm formation is an important virulence factor in *Candida* species. Diverse candida species cause implant-associated infections, in which the fungus forms a biofilm matrix on the surface of catheters, artificial joints, prosthetic heart valves, and other medical devices (30, 31). Although *C. albicans* produces quantitatively more and increasingly complex biofilms than *C. parapsilosis* (17), *C. parapsilosis* bloodstream isolates consistently form biofilms (32), suggesting a correlation between biofilm and *C. parapsilosis* infections. We found that biofilm formation in the *C. parapsilosis* lipase-negative mutant was dramatically reduced. Microscopy findings correlated with the quantitative results, confirming that *C. parapsilosis* WT produced more biofilm than the lipase-negative strain. The mutant strain appeared to form only basal blastospore layers. Notably, the morphology of *C. parapsilosis* biofilms are less complex than biofilms formed by *C. albicans*.

In addition, mutants were tested in different infection models in order to establish the role of lipase in virulence. Recently we described that RE human tissues are extremely useful for modeling host interactions with *C. parapsilosis* and for studying fungal virulence factors (15). We found marked histological differences after challenge of the human oral epithelium tissue multilayers with WT and lipase-negative mutants. Oral epithelium infected with WT *C. parapsilosis* had severe alterations of keratinocytes with disruption of the superficial epithelium and cleft formation between cells associated with increased intracellular edema, atrophy, and apoptosis. In contrast, minimal alterations were apparent in tissues challenged with the lipase-negative strain, which also largely failed to attach to the tissue surface.

Macrophages play an important role in the immunologic response to invading microorganisms, indirectly by processing and presenting antigens to other effector cells and directly by phagocytosing and killing microbial pathogens (33). Our results show that macrophages are able to ingest and kill lipase-negative mutant more efficiently than WT cells. The molecular basis of enhanced phagocytosis and killing of lipase-negative cells by macrophages is not known, but secreted hydrolytic enzymes such as aspartic proteinases can act as cytolysins in macrophages after phagocytosis (10), and our results suggest that secreted lipases may be involved in *C. parapsilosis* survival after phagocytosis.

The lipase-negative strain was less virulent in a murine intraperitoneal infection model. After 4 days of infection, the homozygous lipase-negative cells were cleared from infected mice. However, the fact that mice challenged with the WT strain were also able to clear the pathogen within 7 days after infection underscores the urgent need to develop a new animal model to mimic in vivo *C. parapsilosis* infections. In intraperitoneal infection, *Candida* cells have to penetrate tissue layers to cause invasive disease, a process involving extracellular hydrolytic enzymes (10–12). In contrast, our intravenous infection model bypassed the requirement for invasion

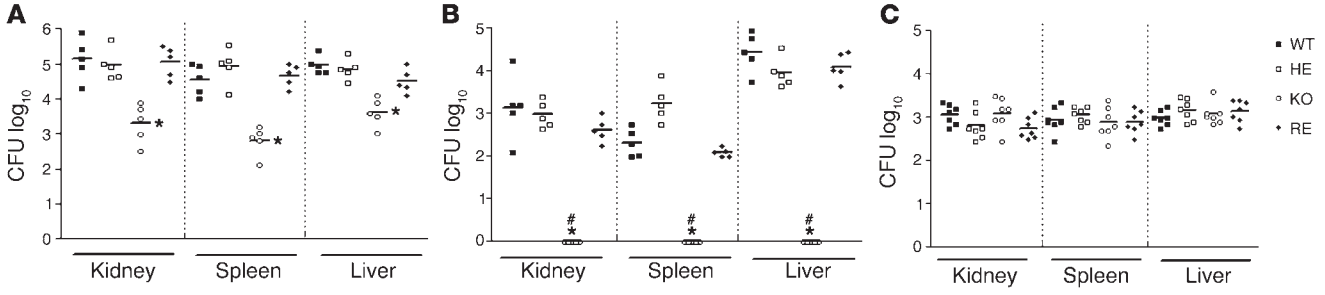

Figure 8
Intraperitoneal and intravenous infection of mice with WT and homozygous Δ*cplip1-2*/Δ*cplip1-2*, heterozygous *CpLIP1-2*/Δ*cplip1-2*, and reconstituted Δ*cplip1-2*/*CpLIP2* mutants. (**A**) CFUs in the kidney, spleen, and liver 2 days after intraperitoneal infection and (**B**) 4 days after infection. (**C**) CFU counts determined from mice intravenously infected in the kidney, spleen, and liver 2 days after infection. Each box represents 1 mouse. *$P \leq 0.0049$ (Kruskal-Wallis); #, no detectable CFU. Data are representative of 2 independent experiments.

Table 1
C. parapsilosis strains constructed and used during this study

C. parapsilosis strains	Genotype
GA1[A]	WT
Lipase mutants	
HebFLP[B]	*CpLIP1-CpLIP2/Δcplip1-Δcplip2::SAT1-FLIP*
He[C]	*CpLIP1-CpLIP2/Δcplip1-Δcplip2::FRT*
KobFLP[D]	*Δcplip1-Δcplip2/Δcplip1-Δcplip2::SAT1-FLIP*
Ko[E]	*Δcplip1-Δcplip2/Δcplip1-Δcplip2::FRT*
Reconstituted mutants	
RebFLP[F]	*Δcplip1-Δcplip2/Δcplip1-Δcplip2/CpLIP2::SAT1-FLIP*
Re[G]	*Δcplip1-Δcplip2/Δcplip1-Δcplip2/CpLIP2::FRT*

[A]Ref. 24. [B]Heterozygous mutant prior to FLP activation; [C]heterozygous mutant; [D]homozygous mutant prior to FLP activation; [E]homozygous mutant; [F]reconstituted isolate prior to FLP activation; [G]reconstituted isolate.

and did not show any significant differences in CFU counts between mice infected with WT and mice infected with gene-deleted mutant cells. The ability of *Candida* cells to damage cultured endothelial cells has been used as an indicator of fungal virulence (18, 34). Our results showed no differences between WT and lipase mutant *C. parapsilosis* in the damage they caused to HUVECs. Interestingly, the damage caused by WT *C. parapsilosis* was 3 times less than that caused by *C. albicans*, supporting the fact that *C. parapsilosis* is inherently less pathogenic in the setting of intact tissues and consistent with the findings of our intravenous infection model.

In conclusion, we have developed an efficient system for targeted gene deletion in *C. parapsilosis* and applied these techniques to a well characterized WT isolate to generate lipase-negative mutants and a RE strain in order to evaluate the contribution of lipase to the pathogenesis of this critically important fungus. Our results show that lipase is an important virulence factor in *C. parapsilosis*, since it is associated with the capacity of the fungus to grow in lipid-rich medium, produce biofilm, and survive in macrophages. The production of lipase is essential for *C. parapsilosis* to attach, invade, and damage RE oral epithelium and to invade host tissues in a murine intraperitoneal infection model. Therefore the lipase of *C. parapsilosis* and perhaps other fungal lipases are new potential targets for the development of antimycotic drugs.

Methods

Microorganisms and cloning vectors. C. parapsilosis strains used or constructed during this study are listed in Table 1. The strains were grown in YPD medium containing 10 g/l yeast extract, 10 g/l peptone, and 20 g/l glucose. Plasmids pCR-BluntII-TOPO (Invitrogen) and pGEM–T (Promega) were used as cloning vectors. Transformed isolates were maintained in YPD containing 100 μg/ml Nou (Werner Bioagents). Nou^R colonies were grown for 24 hours in YNB minimal media (7 g/l YNB without amino acids, 5 g/l ammonium sulfate) containing 20 g/l maltose. After incubation, 10^2 cells were plated on YPD plates containing 20 μg/ml Nou. Nou^S colonies were selected and used for the second round of transformation. *E. coli* DH5α (Fermentas) was used for the propagation of vector molecules and DNA manipulation (35).

Construction of plasmids. To generate lipase-negative mutants from *C. parapsilosis*, we used the *SAT1*-flipper method (16). First we amplified a 3,019-bp fragment from the GA1 genomic DNA with the primers cplfw (5′-TGCCCCAGTTAAACCATCACAA-3′) and cplrev (5′-CTCCCAAAAAGCCATCTCAAG-3′) and cloned it into the vector pGEM-T (Promega), resulting in pCPL. pCPL was digested with *Bgl*II, resulting a 2,701-bp deletion in the cloned genomic fragment. To construct the KO vector pCPLKO, pSFS2, which contains a *C. albicans*–adapted Nou resistance marker *caSAT1* (16), was digested with *Xho*I and *Sac*I to produce the *SAT1* flipper cassette. The fragment was blunt ended and cloned into *Bgl*II digested and blunt ended pCPL resulting in pCPLKO. A fragment excised with *Nco*I and *Sac*I from pCPLKO was used for *C. parapsilosis* transformation.

In order to rescue the wild phenotype in gene-disrupted mutants the vector pCPLRE was constructed. First, pCPL was digested with *Cla*I, then the linearized fragment was blunt ended and the *Xho*I-*Sac*I (blunt end) *SAT1* flipper cassette was ligated to form the reconstruction plasmid pCPLRE. To rescue the lipolytic activity, the linear DNA fragment containing the complete *CpLIP2* open reading frame as well as upstream and downstream sequences derived from pCPLRE was transformed into the homozygous lipase-negative mutants.

Transformation of C. parapsilosis. C. parapsilosis strains were transformed by electroporation as described previously (24), with slight modifications. *C. parapsilosis* GA1 yeast cells were grown overnight in YPD medium at 30°C. The cells were pelleted at 3,000 *g* and suspended in 100 ml TE buffer (10 mM Tris-HCl, 1 mM EDTA, pH 7.5) containing 0.1 M lithium acetate (Sigma-Aldrich). The suspension was incubated in a rotary shaker at 0.75 *g* for 45 minutes at 30°C. After addition of 2.5 ml of 1 M dithiothreitol (Sigma-Aldrich), the suspension was kept in the shaker for additional 15 minutes. Cells were diluted to 100 ml with water, centrifuged, washed twice with ice-cold water and then with 1 M ice-cold sorbitol. The cells were suspended in 1 ml of 1 M sorbitol.

Cells in a total volume of 40 μl were used with or without plasmid DNA for electroporation. The transformation mixture containing 5 μg *Nco*I-*Sac*I digested and purified fragment from plasmids pCPLKO and pCPLRE was transferred to an ice-cold electroporation cuvette (0.2-cm gap) (Bio-Rad) and pulsed at 1.5 kV, 25 μF, 200 Ω in a Bio-Rad electroporator. Cells were immediately suspended in YPD containing 1 M sorbitol and incubated at 30°C for 4 hours before plating on selection YPD plates supplemented with 100 μg/ml Nou. Nou^R colonies were picked after 48 hours of growth and cultured in YPD liquid medium containing 100 μg/ml Nou.

Nucleic acid isolation and hybridization. Standard methods (24) were used for DNA isolation, gel electrophoresis, and Southern blotting. Approximately 5 μg genomic DNA isolated from *C. parapsilosis* was digested with *Pac*I and *Avr*II, separated on a 1% agarose gel, transferred onto nylon membrane (Roche), and fixed by UV crosslinking. Labeling of the 442-bp cplip probe using primers cplipsfw (5′-ACCTCATTTGTGTTCTCCTG-3′) and cplipsrev (5′-GGTTGTCCATCATCATCGTGTT-3′) and subsequent hybridization of the membranes at 68°C were carried out using the DIG DNA Labeling and Detection Kit (Roche) following the manufacturer's instructions.

Determination of lipolytic activity. Lipolytic activities were examined using colonies grown on rhodamine B plates (29) with certain modifications (7 g/l YNB, 20 ml/l olive oil, 50 ml/l FBS, 1 ml/l 1 M rhodamine B). Additionally, lipolytic activities of supernatants of overnight cultures shaken in intralipid medium, a lipid-rich solution, and in YNB–olive oil medium at 0.8 *g* and 30°C were measured with a lipase assay using paranitrophenyl palmitate (pNPP; Sigma-Aldrich) (36) and using naphthyl palmitate as substrate (37) with the following modification: 200 μl culture supernatants were added to 800 μl lipase assay buffer (1.12 mM α-naphthylpalmitate, 14 mM citric acid, 74 mM Tris buffer, pH 5.5) and incubated for 1 hour at 37°C. The reaction was terminated by the addition of 0.5 ml of 0.5 N NaOH solution. The released α-naphthol was measured with Fast Violet B (Sigma-Aldrich), and the absorbance was determined at 520 nm.

Growth assays. Growth of the WT *C. parapsilosis* strain GA1 and the constructed mutants was analyzed in liquid YPD, YNB, and YNB–olive oil (7 g/l YNB without amino acids, 5 g/l ammonium sulfate, or 20 ml/l olive oil, sterile filtered) media that were inoculated with 10^6 cells/200 μl

medium and incubated at 30°C. Cell numbers were determined by hemocytometer at different intervals. Growth was similarly examined in lipid-rich intralipid media (7 g/l YNB without amino acids, 5 g/l ammonium sulfate, 50 ml/l intralipid [Sigma-Aldrich]), sterile filtered except growth was assessed by CFU determination by plating on YPD agar.

Biofilm formation. For biofilm formation, polystyrene and polyethylene 96-well plates were obtained from Fisher Scientific, and silicone elastomer sheets were obtained from Bentec Medical Corp. The latter was chosen due to its similarity to material used in indwelling devices, its availability as flat medical-grade sheeting (which is not the case for materials such as catheter-grade polyvinyl chloride), and the documented ability of silicone elastomer to promote *Candida* biofilm formation (17). *C. parapsilosis* cells were collected by centrifugation, washed twice with PBS, counted using a hemocytometer, and suspended at 10^7 cells/ml in YNB medium. Polystyrene and polyethylene 96-well plates and silicone sheets were incubated with 100 μl FBS overnight and washed twice with sterile PBS, and 100 μl suspensions of yeast were incubated at 37°C without shaking for 48 hours. The wells were washed 3 times with 0.05% Tween-20 in Tris-buffered saline to remove nonadhered cells. Fungal cells that remained attached to the plastic surface were considered to have formed into biofilm.

Measurement of biofilm metabolic activity by the XTT reduction assay. A semiquantitative measurement of *C. parapsilosis* biofilm formation was obtained from the 2,3-bis(2-methoxy-4-nitro-5-sulfophenyl)-5-[(phenylamino) carbonyl]-2H-tetrazolium hydroxide (XTT) reduction assay (38). For the WT and mutant strains, 50 μl of XTT salt solution (1 mg/ml in PBS) and 4 μl of menadione solution (1 mM in acetone; Sigma-Aldrich) were added to each well containing *C. parapsilosis* biofilm. Microtiter plates were incubated at 37°C for 5 hours. The colorimetric change was measured using a microtiter reader (Labsystem Multiskan MS) at 492 nm. In all of the experiments, microtiter wells containing heat-killed *C. parapsilosis*, minimal medium alone, were included as negative controls.

Microscopy of biofilm. Microscopic examinations of biofilms were performed with light microscopy using an Axiovert 200 M inverted microscope (Zeiss). For confocal microscopy analysis *C. parapsilosis* biofilms were grown in 96-well microtiter plates containing minimal medium for 48 hours. Wells containing mature biofilms were washed 3 times with PBS and incubated for 45 minutes at 37°C in 75 μl of PBS containing the fluorescent stains FUN-1 (10 μM) and ConA–Alexa Fluor 488 conjugate. FUN-1 (excitation wavelength, 470 nm; emission, 590 nm) converts to orange-red cylindrical intravacuolar structures by metabolically active cells, while ConA (excitation wavelength, 488 nm; emission, 505 nm) binds to glucose and mannose residues of cell wall and emits green fluorescence. Microscopic examinations of biofilms were performed with confocal microscopy using an Axiovert 200 M inverted microscope. The objective used was ×20. Depth measurements were taken at regular intervals across the width of the device. To determine the structure of the biofilms, a series of horizontal (*x-y*) optical sections with a thickness of 1 μm were taken throughout the biofilm. Confocal images of green (ConA) and red (FUN-1) fluorescence were conceived simultaneously using a multichannel mode. Z-stack images and measurements were corrected utilizing AxioVision 4.4 software, deconvolution mode (Zeiss).

Phagocytosis and killing of C. parapsilosis by macrophages. The macrophage-like cell lines J774.16 and RAW 264.7 were used to study phagocytosis and phagocytic killing. The cells were cultured in DMEM with 10% heat-inactivated FCS, 10% NCTC-109 medium, and 1% nonessential amino acids. All macrophages were plated at 10^5 cells per well in an 8-chamber polystyrene tissue culture glass slide (BD) and grown overnight before use in the phagocytosis assays.

Phagocytosis assays with *C. parapsilosis* were done according to previously described protocol (39, 40). *C. parapsilosis* cells were collected after 24 hours of growth and washed 3 times in PBS. Yeast cells were added to the macrophage monolayer at an effector/target ratio of 1:15, and the suspension was incubated at 37°C for 1 hour. Cocultures were then washed with HBSS (pH 7.2), and the slides were stained with 0.01% acridine orange (Sigma-Aldrich) for 45 seconds by the method of Pruzanski and Saito (41). The slides were gently washed with HBSS and stained for 45 seconds with 0.05% crystal violet (Sigma-Aldrich) dissolved in 0.15 M NaCl. Finally, the slides were rinsed 3 times with PBS, mounted on microscope coverslips, and sealed at the edge with nail polish. The phagocytic index was determined by fluorescence microscope (Axiovert 200 M inverted microscope; Zeiss). For each experiment 3 fields in each well were counted, and at least 200 macrophages were analyzed in each well. The phagocytic index was the ratio of the number of intracellular yeast cells to the number of macrophages counted.

Colony counts were made to determine the number of viable *C. parapsilosis* yeast cells after phagocytosis. For CFU determination J774.16 and RAW 264.7 macrophages were infected with *C. parapsilosis* cells as described above. After 2 hours of incubation, macrophage cells were lysed by forcibly pulling the culture through a 26-gauge needle 5 times. The lysates were serially diluted and plated on Sabouraud dextrose agar at 37°C. CFU determinations were made after 72 hours. Controls also consisted of yeast grown without macrophages. All tests were preformed in triplicate.

Endothelial cell damage assay. HUVECs were grown in M199 (Sigma-Aldrich) supplemented with 10% FBS and 2 mM L-glutamine. For use in damage assays, HUVECs were grown on a collagen matrix in 96-well tissue culture plates (Fisher Scientific) to create confluent layers. All incubations were at 37°C in 5% CO_2. Endothelial cell damage caused by *C. parapsilosis* WT and mutants was quantified by a method described by Filler et al. (18) and modified by Crowe et al. (34). LDH release from HUVEC monolayers was measured after challenge with *C. parapsilosis* cells. *C. albicans* SC5314 was used as a positive control. An inoculum of yeast cells was grown at 37°C for 24 hours in YNB with 2% glucose and washed twice in PBS. The yeast cells were applied to confluent HUVEC monolayers in a 96-well plate in a 150-μl sample volume containing 1.6×10^5 yeast cells. Growth medium alone was added to control wells with and without HUVEC layers. The plate was incubated at 37°C with 5% CO_2 for 3 hours. Maximal LDH release was obtained in a control set of wells by adding 15 μl of 0.9% Triton X-100 to each well and vigorously disrupting the HUVEC layers with a pipette tip 45 minutes before the end of the 8-hour incubation period; background LDH release was that from nondisrupted HUVEC layers. Samples (50 μl) were taken from each well, and LDH was assayed spectrophotometrically at 492 nm using the CytoTox96 kit (Promega) according to the manufacturer's instructions. The percentage lysis of HUVECs challenged with *C. parapsilosis* and *C. albicans* cells was calculated as: experimental LDH release − background/mean maximal LDH release − background. All experiments were performed with 4 replicate wells of 3 independent experiments.

In vitro infection model using RE human oral epithelium. We utilized our in vitro infection model as described previously (15). RE human oral epithelium was obtained from SkinEthic Laboratory and infected with 2×10^6 yeast cells in 100 μl PBS by adding the cell suspension to the 1-ml cell culture medium. Control cultures were grown in medium with 100 μl PBS added. The infected and control cultures were incubated at 37°C with 5% CO_2 at 100% humidity for 48 hours.

LDH measurement. The release of LDH from cells into the medium was monitored as a measure of cell damage. LDH in medium from cultures containing uninfected and infected tissues was measured at 24 hours and 48 hours by CytoTox-ONE kit (Promega) according to the manufacturer's instructions. *Candida* cells alone incubated under identical conditions were included as negative controls. The LDH released in the presence of different *Candida* isolates was expressed relative to the untreated control tissue with the LDH activity of *Candida* cells alone subtracted from the LDH of the tissue plus the fungi.

Mouse infection models. Intravenous infections were carried out by injecting 10^7 fungal cells in 100 μl PBS into the tail vein of Balb/c mice (female, 6–8 weeks of age; obtained from the National Cancer Institute). Animal care for this study was approved by the institutional animal care and use committee of Albert Einstein College of Medicine of Yeshiva University. CFU numbers were determined from the liver, kidneys, and spleen 2 and 4 days after infection by plating tissue homogenates on YPD agar. Balb/c mice were also inoculated intraperitoneally with 10^7 cells of WT or mutant strains. Mice were sacrificed 48 and 96 hours after the infection, and CFUs were determined.

Statistics. Murine experiments were powered for significance. All other experiments were performed in triplicate, and each value is shown as the mean ± SD. The significance of differences between sets of data was determined by 2-tailed Student's *t* test, Kruskal-Wallis test, or ANOVA according to the data type.

Acknowledgments

The authors would like to thank Joachim Morschhäuser for providing the pSFS2 plasmid. J.D. Nosanchuk is supported in part by NIH grants AI52733 and AI056070-01A2, a Wyeth Vaccine Young Investigator Research Award from the Infectious Disease Society of America, and the Center for AIDS Research at the Albert Einstein College of Medicine and Montefiore Medical Center (NIH grant AI-51519).

Received for publication April 3, 2007, and accepted in revised form June 20, 2007.

Address correspondence to: Attila Gácser, Albert Einstein College of Medicine, 1300 Morris Park Avenue, Bronx, New York 10461, USA. Phone: (718) 430-2993; Fax: (718) 430-8968; E-mail: gacsera@gmail.com.

1. Fridkin, S.K., Kaufman, D., Edwards, J.R., Shetty, S., and Horan, T. 2006. Changing incidence of *Candida* bloodstream infections among NICU patients in the United States:1995-2004. *Pediatrics.* **117**:1680–1687.
2. Krcmery, V., et al. 2000. Fungemia in neonates: report of 80 cases from seven University hospitals. *Pediatrics.* **105**:913–914.
3. Pagano, L., et al. 1999. Retrospective study of candidemia in patients with hematological malignancies. Clinical features, risk factors and outcome of 76 episodes. *Eur. J. Haematol.* **63**:77–85.
4. Pfaller, M.A., et al. 1998. International surveillance of bloodstream infections due to *Candida* species: frequency of occurrence and antifungal susceptibilities of isolates collected in 1997 in the United States, Canada, and South America for the SENTRY Program. The SENTRY Participant Group. *J. Clin. Microbiol.* **36**:1886–1889.
5. Pfaller, M.A., et al. 2001. International surveillance of bloodstream infections due to *Candida* species: frequency of occurrence and in vitro susceptibilities to fluconazole, ravuconazole, and voriconazole of isolates collected from 1997 through 1999 in the SENTRY antimicrobial surveillance program. *J. Clin. Microbiol.* **39**:3254–3259.
6. Benjamin, D.K., Jr., Garges, H., and Steinbach, W.J. 2003. *Candida* bloodstream infection in neonates. *Semin. Perinatol.* **27**:375–383.
7. Clerihew, L., Lamagni, T.L., Brocklehurst, P., and McGuire, W. 2007. *Candida parapsilosis* infection in very low birthweight infants. *Arch. Dis. Child. Fetal Neonatal Ed.* **92**:F127–F129.
8. Bramono, K., Yamazaki, M., Tsuboi, R., and Ogawa, H. 2006. Comparison of proteinase, lipase and alpha-glucosidase activities from the clinical isolates of *Candida* species. *Jpn. J. Infect. Dis.* **59**:73–76.
9. Hube, B., et al. 2000. Secreted lipases of *Candida albicans*: cloning, characterisation and expression analysis of a new gene family with at least ten members. *Arch. Microbiol.* **174**:362–374.
10. Monod, M., and Borg-von, Z.M. 2002. Secreted aspartic proteases as virulence factors of *Candida* species. *Biol. Chem.* **383**:1087–1093.
11. Stehr, F., et al. 2004. Expression analysis of the *Candida albicans* lipase gene family during experimental infections and in patient samples. *FEMS Yeast Res.* **4**:401–408.
12. Schaller, M., Borelli, C., Korting, H.C., and Hube, B. 2005. Hydrolytic enzymes as virulence factors of *Candida albicans*. *Mycoses.* **48**:365–377.
13. Neugnot, V., Moulin, G., Dubreucq, E., and Bigey, F. 2002. The lipase/acyltransferase from *Candida parapsilosis*: molecular cloning and characterization of purified recombinant enzymes. *Eur. J. Biochem.* **269**:1734–1745.
14. Brunel, L., et al. 2004. High-level expression of *Candida parapsilosis* lipase/acyltransferase in Pichia pastoris. *J. Biotechnol.* **111**:41–50.
15. Gacser, A., Schaefer, W., Nosanchuk, J.S., Salomon, S., and Nosanchuk, J.D. 2007. Virulence of *Candida parapsilosis*, *Candida orthopsilosis*, and *Candida metapsilosis* in reconstituted human tissue models. *Fungal Genet. Biol.* In press.
16. Reuss, O., Vik, A., Kolter, R., and Morschhauser, J. 2004. The SAT1 flipper, an optimized tool for gene disruption in *Candida albicans*. *Gene.* **341**:119–127.
17. Kuhn, D.M., Chandra, J., Mukherjee, P.K., and Ghannoum, M.A. 2002. Comparison of biofilms formed by *Candida albicans* and *Candida parapsilosis* on bioprosthetic surfaces. *Infect. Immun.* **70**:878–888.
18. Filler, S.G., Swerdloff, J.N., Hobbs, C., and Luckett, P.M. 1995. Penetration and damage of endothelial cells by *Candida albicans*. *Infect. Immun.* **63**:976–983.
19. Brito, L.R., et al. 2006. Clinical and microbiological aspects of candidemia due to *Candida parapsilosis* in Brazilian tertiary care hospitals. *Med. Mycol.* **44**:261–266.
20. Rodero, L., et al. 2005. Multicenter study of fungemia due to yeasts in Argentina [In Spanish]. *Rev. Argent. Microbiol.* **37**:189–195.
21. Weems, J.J., Jr. 1992. *Candida parapsilosis*: epidemiology, pathogenicity, clinical manifestations, and antimicrobial susceptibility. *Clin. Infect. Dis.* **14**:756–766.
22. Fundyga, R.E., Kuykendall, R.J., Lee-Yang, W., and Lott, T.J. 2004. Evidence for aneuploidy and recombination in the human commensal yeast *Candida parapsilosis*. *Infect. Genet. Evol.* **4**:37–43.
23. Nosek, J., et al. 2002. Genetic manipulation of the pathogenic yeast *Candida parapsilosis*. *Curr. Genet.* **42**:27–35.
24. Gacser, A., Salomon, S., and Schafer, W. 2005. Direct transformation of a clinical isolate of *Candida parapsilosis* using a dominant selection marker. *FEMS Microbiol. Lett.* **245**:117–121.
25. Hube, B., and Naglik, J. 2001. *Candida albicans* proteinases: resolving the mystery of a gene family. *Microbiology.* **147**:1997–2005.
26. Jaeger, K.E., et al. 1994. Bacterial lipases. *FEMS Microbiol. Rev.* **15**:29–63.
27. Saiman, L., et al. 2000. Risk factors for candidemia in Neonatal Intensive Care Unit patients. The National Epidemiology of Mycosis Survey study group. *Pediatr. Infect. Dis. J.* **19**:319–324.
28. Wanten, G.J., et al. 2002. Parenteral administration of medium- but not long-chain lipid emulsions may increase the risk for infections by *Candida albicans*. *Infect. Immun.* **70**:6471–6474.
29. Kouker, G., and Jaeger, K.E. 1987. Specific and sensitive plate assay for bacterial lipases. *Appl. Environ. Microbiol.* **53**:211–213.
30. Donlan, R.M. 2001. Biofilm formation: a clinically relevant microbiological process. *Clin. Infect. Dis.* **33**:1387–1392.
31. Douglas, L.J. 2003. *Candida* biofilms and their role in infection. *Trends Microbiol.* **11**:30–36.
32. Song, J.W., et al. 2005. Differences in biofilm production by three genotypes of *Candida parapsilosis* from clinical sources. *Med. Mycol.* **43**:657–661.
33. Lorenz, M.C., and Fink, G.R. 2002. Life and death in a macrophage: role of the glyoxylate cycle in virulence. *Eukaryot. Cell.* **1**:657–662.
34. Crowe, J.D., et al. 2003. *Candida albicans* binds human plasminogen: identification of eight plasminogen-binding proteins. *Mol. Microbiol.* **47**:1637–1651.
35. Sambrook, J., Fritsch, E.F., and Maniatis, T. 1989. *Molecular cloning: a laboratory manual*. 2nd edition. Cold Spring Harbor Laboratory Press. Cold Spring Harbor, New York, USA. 1659 pp.
36. Voigt, C.A., Schafer, W., and Salomon, S. 2005. A secreted lipase of *Fusarium graminearum* is a virulence factor required for infection of cereals. *Plant J.* **42**:364–375.
37. Ran, Y., Yoshiike, T., and Ogawa, H. 1993. Lipase of *Malassezia furfur*: some properties and their relationship to cell growth. *J. Med. Vet. Mycol.* **31**:77–85.
38. Martinez, L.R., and Casadevall, A. 2006. Susceptibility of *Cryptococcus neoformans* biofilms to antifungal agents in vitro. *Antimicrob. Agents Chemother.* **50**:1021–1033.
39. Takao, S., et al. 1996. Role of reactive oxygen metabolites in murine peritoneal macrophage phagocytosis and phagocytic killing. *Am. J. Physiol.* **271**:C1278–C1284.
40. Owaki, T., et al. 2000. Endothelial cells potentiate phagocytic killing by macrophages via platelet-activating factor release. *Am. J. Physiol. Heart Circ. Physiol.* **278**:H269–H276.
41. Pruzanski, W., and Saito, S. 1988. Comparative study of phagocytosis and intracellular bactericidal activity of human monocytes and polymorphonuclear cells. Application of fluorochrome and extracellular quenching technique. *Inflammation.* **12**:87–97.